ALDH2 Repression Promotes Lung Tumor Progression via Accumulated Acetaldehyde and DNA Damage[1]

Kaimi Li[*,†,2], Wenzheng Guo[*,†,2], Zhanming Li[‡,2], Yang Wang[§], Beibei Sun[¶], Dongliang Xu[*,†], Jing Ling[§], Hongyong Song[*,†], Yueling Liao[*,†], Tong Wang[*,†], Bo Jing[*,†], Min Hu[*,†], Yanbin Kuang[#], Qi Wang[#], Feng Yao[**], Aijun Sun[††], Liang Zhu[§], Lishun Wang[‡] and Jiong Deng[*,†,‡‡]

[*]Key Laboratory of Cell Differentiation and Apoptosis of Chinese Minister of Education, Shanghai General Hospital, Shanghai Jiao Tong University School of Medicine, Shanghai, China; [†]Shanghai Key Laboratory for Tumor Microenvironment and Inflammation, Shanghai General Hospital, Shanghai Jiao Tong University School of Medicine, Shanghai, China; [‡]Institute of Fudan-Minhang Academic Health System, Minhang Hospital, Fudan University, 170 Xinsong Road, Shanghai 201199, China; [§]Department of Pharmacology and Chemical Biology, Shanghai General Hospital, Shanghai Jiao Tong University School of Medicine, Shanghai, China; [¶]Translational Medical Research Center, Shanghai Chest Hospital, Shanghai Jiao Tong University, Shanghai, China; [#]Department of Respiratory Medicine, The Second Affiliated Hospital, Dalian Medical University, Dalian, China; [**]Department of Thoracic Surgery, Shanghai Chest Hospital, Shanghai Jiao Tong University, Shanghai, China; [††]Institute of Biomedical Sciences, Fudan University, Shanghai, China; [‡‡]Department of Oncology, Shanghai General Hospital, Shanghai Jiao Tong University School of Medicine, Shanghai, China

Abstract

The major role of aldehyde dehydrogenase 2 family (ALDH2) is to detoxify acetaldehyde (ACE) to non-toxic acetic acid. Many evidences suggest that ALDH2 dysfunction contributes to a variety of human diseases including cancer. However, the biological function and molecular mechanism of ALDH2 in tumor progression remain elusive. In this study, we found that ALDH2 repression was associated with poor prognosis in lung adenocarcinoma. Overexpression of ALDH2 inhibited malignant features of lung adenocarcinoma cells, such as proliferation, stemness and migration, whereas ALDH2 knockdown increased these features. Mechanistically, ALDH2 repression led to accumulation of ACE; whereas ACE enhanced the migration features of lung adenocarcinoma cells, which was associated with increased DNA damage. Importantly, accumulated ACE and increased DNA damage were identified in Aldh2-knockout (KO) mouse lung tissues in vivo. Consistent with this concept, treatment of lung adenocarcinoma cells with ALDH2 agonist Alda-1 suppressed the proliferation,

stemness and migration features of lung adenocarcinoma cells. Thus, activating ALDH2, such as via its agonist, may provide a novel strategy for treatment of lung cancer.

Introduction

Lung cancer is the leading cause of cancer-related death worldwide [1,2]. The progression of lung cancer has been linked to increased genomic instability, which could be induced by various factors including cigarette smoking, DNA damaging, toxic chemicals, reactive oxygen species (ROS) and cytotoxic metabolites [3,4]. However, the function of these factors in tumor progression remains unclear and the related studies are also limited. Identification of the roles and regulatory pathways of these factors in tumor progression may thus help to provide novel approaches for cancer therapy.

Endogenous aldehydes and acetaldehyde (ACE) are abundant molecules within cells, mainly produced by the cellular processing of alcohol and also as an intermediate in sugar metabolism [5]. Aldehydes and ACE are highly reactive molecules, generating a range of DNA modification products including DNA strand crosslinks and DNA-protein crosslinks. Due to their toxicity, aldehydes are detoxified by enzymes such as aldehyde dehydrogenase 2 family (ALDH2), which oxidizes ACE to acetate [6]. ALDH2, a mitochondria enzyme, is a member of the aldehyde dehydrogenase (ALDH) superfamily that has 19 ALDH subtypes, ALDH2 is mainly responsible for detoxification of ACE derived from ethanol metabolism in the liver. ALDH2 can also detoxify reactive aldehydes derived from drugs, food, spices, and from endogenous metabolism in other tissues. Clinically, ALDH2 dysfunction contributes to a variety of human diseases including cardiovascular diseases, diabetes, neuro-degenerative diseases, stroke, and cancer [7,8]. Repression of ALDH2 is associated with the induction of cytotoxicity, DNA damage and oncogenic effects in several types of tumors [9,10]. Recently, it has been shown that alcohol and endogenous aldehyde damage chromosomes and mutate stem cells [11]. Moreover, chromosomal instability promotes cancer metastasis via cytosolic DNA derived from genomic DNA rupture [12]. Taken together, these observations raise a question whether ALDH2-deficiency affects the malignant features of lung cancers via accumulated ACE. However, the roles and molecule mechanism of ALDH2 and ACE in lung cancer remain unknown. In this study, we investigated the function of ALDH2 in lung adenocarcinoma and found that ALDH2 repression led to increased malignant features. Moreover, the migration capacity is regulated by accumulated ACE and DNA damage.

Materials and Methods

Western Blot

To prepare whole-cell or tissue extracts, cells or tissues were lysed by RIPA lysis buffer (150 mM NaCl,1% Nonidet P-40, 0.1% SDS, 0.5% deoxycholate, 50 mM Tris (pH 8.0), 25 mM NaF, 2 mM Na3VO4, 5 mM PMSF and2 mg/mL of aprotinineen (0.2% v/v) containing 5% bovine serum albumin (BSA). Antibodies against ALDH2 (Abcam, ab108306), vinculin (Santa, sc-73,264), γH2AX (CST, 9718P), CD44 (CST, 3570), STING (Abcam, ab92605) and β-actin (MBL, PM053–7) were used. The secondary antibody was goat anti-rabbit or anti-mouse horseradish peroxidase (HRP)-conjugated IgG. All antibodies were diluted according to manufacturers' instructions. ECL kit (Millipore) was used to detect the protein bands.

Cell Lines and Cell Culture

Human embryonic kidney cells (HEK293T) and Human lung adenocarcinoma cell lines were obtained from American Type Culture Collection (ATCC) and were authenticated by DNA typing at Shanghai Jiao Tong University Analysis Core.

The HEK293T cells and 16HBE (Human bronchial epithelial cells) cells were cultured in DMEM essential medium with 10% fetal bovine serum (FBS). HBEC cells were cultured with serum-free medium, and all other cells were cultured in RPMI-1640 essential medium supplemented with 10% FBS. All cells were cultured in a humidified incubator (37°C, 5% CO_2).

Transfections and Viral Infections

HEK293T cells were transfected with lenti-shALDH2 (or nonspecific sequence) plasmid or lenti-ALDH2 (or GFP) plasmid used for virus production for ALDH2 knock down or overexpression. Lipofectamine 2000 (plasmid: lipo2000 1:4) was used as transfection reagent. The medium was replaced after 4-6 h. Then the lentivirus medium was collected to infect lung adenocarcinoma cells after 48 h. The stably transfected cells were selected by puromycin (2 μg/ml) or blasticidin (10 μg/ml). Then, the cells were expanded and collected for subsequent analysis.

Quantitative Real-Time (Q)-PCR

Human lung cancer tissues were obtained from Shanghai Chest Hospital, Shanghai Jiao Tong University (Shanghai, CHINA). The tissue samples were lysed using Trizol. Then, total RNA was extracted with RNA Extract Kit (TIANGEN, Cat: #RK123) and cDNA were prepared from 1.5 μg total RNA using Fast Quant Kit. The Q-PCR analysis was performed on ABI 7300 real-time PCR machine. All Ct values were standardized by β-actin's Ct value. And the following primers were used:

ALDH2	F: 5′-CCTCACCGCCCTCTATGTG-3′
	R:5′-CGGCCAATCTCAGTGGAGC-3′
β-Actin	F: 5′- GCTCTTTTCCAGCCTTCCTT-3′
	R: 5′-CTTCTGCATCCTGTCAGCAA-3′

Colony Formation Assay

Five hundred cells were seeded on 6 cm-dish in 3 mL culture medium. After being cultured in 37°C for 15 days, the colonies were stained with 0.1% crystal violet at room temperature for 1 h. Then the dishes were photographed and the colony numbers were counted.

Sphere Culture Assay

The lung adenocarcinoma cells were resuspended in culture medium and were put into low-adhered dishes in order to simulate a 3D culture room. Every well of 24-well plate were seeded 10,000 cells. The medium was changed every 3 days. The spheroids size should be taken care to avoid necrosis in the center of the spheres. The spheres were photographed and counted under microscope (Nikon ECLIPSE) after 2 weeks.

Tumorigenicity in Nude Mice

Eight-week-old nude mice were injected subcutaneously with A549-sh-NS/sh-ALDH2 (1.0×10^6) cells combined with matrigel. Three weeks later, the volume of tumors was measured three times per week and further analyzed. The nude mice were obtained from Shanghai Jiao Tong University, School of Medicine Animal Care [experimental animal use permission No: SYXK (Shanghai) 2008–0050] and were maintained in the specific pathogen-free animal facility in the university. Aldh2 knockout (KO) mice were obtained from Aijun Sun's Lab. Animal studies were conducted following the guidelines of the experimental animal ethics committee of Shanghai Jiao Tong University School of Medicine and were approved by the experimental animal ethics committee of Shanghai Jiao Tong University School of Medicine (Shanghai, China).

Side Population Assay

The cultured cells were detached with trypsin and resuspended in RPMI-1640 culture medium supplemented with 2% FBS, and the cell suspension was adjusted to a density of about 1×10^6/ml. Samples were separated to the control group and the experimental group. All samples were stained with Hoechst-33,342 (5 µg/ml). The control group was also added verapamil (50 µM) or Ko143 (5 µM) to inhibit the efflux of the dye by blocking ABCB1 transporters or ABCG2 transporters for gating SP cells. All samples incubated in water at 37°C for 120 mins. In this period, shook the incubation tubes several times. Next, the samples were immediately centrifuged at 4°C and resuspended in ice-cold Hank's Buffer. Propidium iodide (PI, 2 µg/ml) was added to gate out the dead cells. Then the cell suspension was filtered through a 40 µm cell strainer (BD Biosciences, Franklin Lakes, NJ, USA) to obtain a single suspension of cells. Flow cytometry analysis were conducted on Beckman Coulter CytoFLEX

S. Hoechst-33,342 was excited by ultraviolet laser. Finally, the data was analyzed in the CytExpert software.

Flow Cytometry Analysis of CD44 Positive and CD24 Negative Population

The lung adenocarcinoma cells cultured in 6 cm-dish were collected and washed two times using PBS. Then the cells were incubated in 400 µl RPMI-1640 containing 1% CD44-APC, CD24-PE (BD Pharmingen) at 4°C for 30mins, whereas the control were incubated with IgG. The cells were suspended in 400 µl PBS for Flow Cytometry analysis after incubation. The gates were established using the negative control cells stained with IgG. Finally, the data was analyzed in the Flowjo 7.6.1software.

Wound Healing Test

The same amounts of cells were seeded on six-well dishes. When the cells were grown to 90%, scratched a wound at the bottom of the dishes using a pipette tip. Changed the medium and took pictures by an inverted microscope. Then the wounds were photographed every 6 h.

Transwell Assay

The A549-GFP and A549-ALDH2 cells were seeded on the top well of the transwell chambers (Costar) at a density of 2×10^4/well. A total of 1 ml of the conditional medium was added in the bottom chamber. Following cultivation for 24 h, the top well surface of the filter was wiped with a cotton swab to remove the cells. Then the migrated cells were fixed with 4% paraformaldehyde for 20mins. Lastly, the cells were stained with 0.1% crystal violet for 1 h after washing. The migrated cells were observed and captured by an inverted microscope.

Quantification of ACE

800 µl 80% acetonitrile and 200 µl dinitrophenylhydrazine was added to lung tissue samples. Then the tissues were homogenized three times at 5500 rpm for 20s using Bertin Precellys 24 Dual Multifunctional sample homogenizer. After placed in –80°C for 1 h and in room temperature for 4 h, the tissue homogenate was derivatization. After centrifuged at 20000 g for 10 mins, the supernatant was taken for vacuum drying. Finally, 200 µl acetonitrile was added to reconstitute the samples for LC–MS (AB SCIEX 4000) analysis. For the cell samples detection, 80% methanol was used as extraction reagent. The other steps are the same as the tissue extraction method.

Comet Assay

The A549-GFP and A549-ALDH2 cells were treated with 4 mM ACE for two days. Then the cells were harvested and mixed with low-melt agarose (0.5%) at a ratio of 1:10(v/v) and pipetted onto glass slides. After placed at 4°C in the dark for 30mins, the slides were immersed into lysis buffer(100 mM EDTA,2.5 M NaCl,10 mM

Figure 1. ALDH2 repression is associated with poor prognosis in human lung adenocarcinoma. **A.** The mRNA expression of ALDH2 across all tumor samples and paired normal tissues in the Gene Expression Profiling Interactive Analysis (GEPIA) dataset. The histogram represents the median expression of ALDH2 mRNA in tumor and normal tissues. LUAD (lung adenocarcinoma) and LUSC (lung squamous cell carcinoma) were marked in red. **B.** Q-PCR analysis of ALDH2 in tumors and adjacent normal tissues of 16 lung adenocarcinoma patients. **C.** The overall survival (%) curves of lung adenocarcinoma patients with low or high ALDH2 expression. mRNA data was obtained from the Cancer Genome Atlas (TCGA) dataset. According to the mRNA level of ALDH2, patients are classified as ALDH2 high expression group (n = 200) and ALDH2 low expression group (n = 200). log-rank test p value = .0318. **D.** The overall survival (%) curves of lung adenocarcinoma patients with low or high ALDH2 expression from The Human Protein Atlas (THPA) dataset. **E.** Analysis of ALDH2 mRNA expression in lung adenocarcinoma tissues with different pathological stages in University of California Santa Cruz (UCSC) Xena dataset. *t* Test *P* = .0172 ("Stage I" vs. "Stage IV"); *t* test *P* = .0168 ("Stage I vs. "Stage II"); *t* Test *P* = .0377 ("Stage I" vs. "Stage III") *P < .05.

Tris,1% Triton X-100, 10% DMSO) at 4°C for 1 h. Put the slides into alkaline buffer solution (300 mM NaOH, 1 mM EDTA, pH> 13) for 1 h to unwind DNA and then electrophoresed for 30mins in 25 V. Gently immersed slides into neutralizing buffer (0.4 M Tris, pH 7.5) for 5mins and then immersed into 70% ethanol for 5mins. Dried samples completely at room temperature overnight. Placed SYBR Green onto each sample for 30mins. The slides were observed and photographed by epifluorescence microscopy.
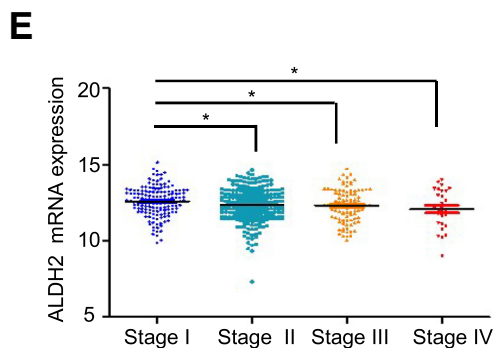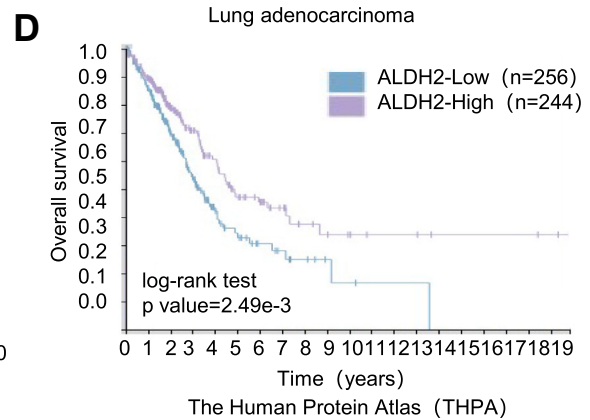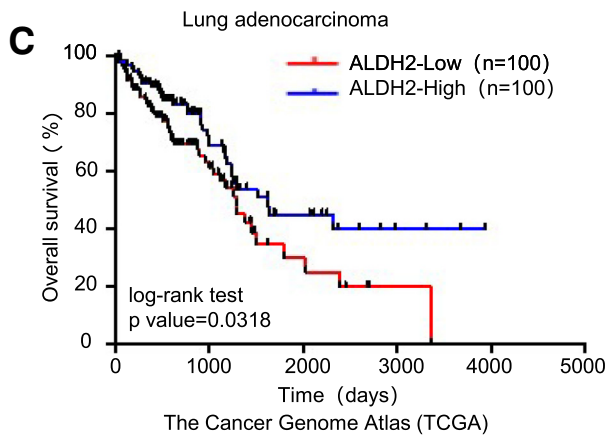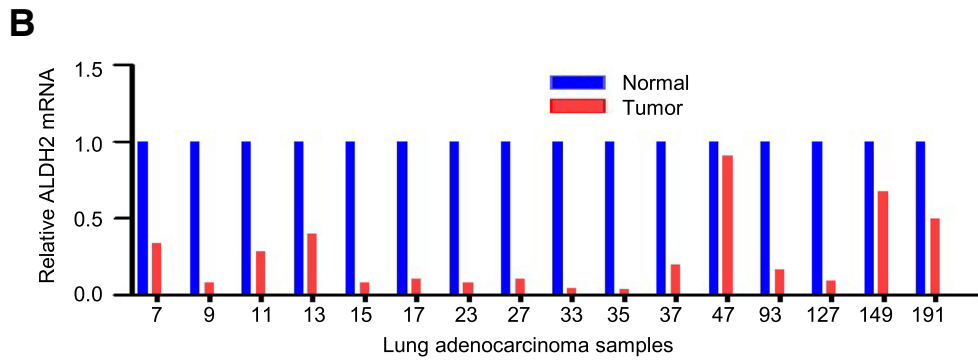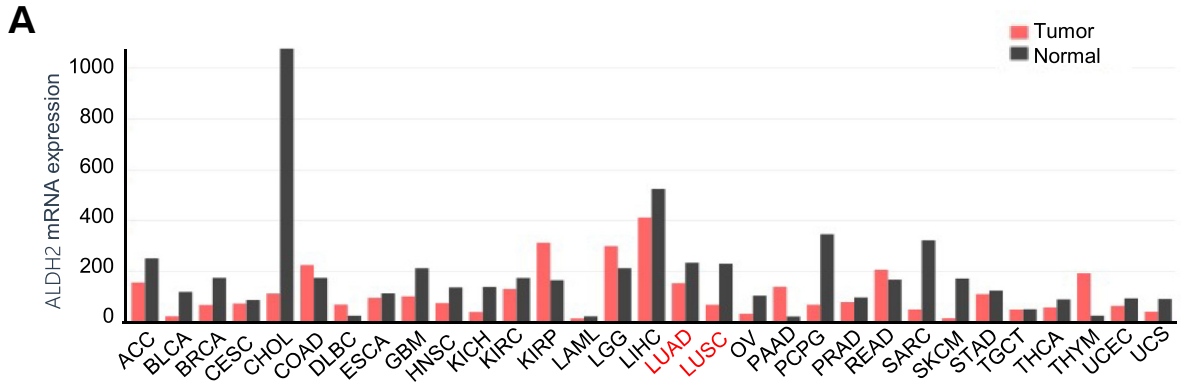
HE Staining

Dewaxed the paraffin slices using xylene and gradient Ethanol. Then immersed the slices into hematoxylin for 3-8mins to stain the nucleus and washed with water. Following stained with 0.6% ammonia water, rinsed with running water. Next, put the slices into Eosin staining solution for 1-3mins to stain cytoplasm. At last,
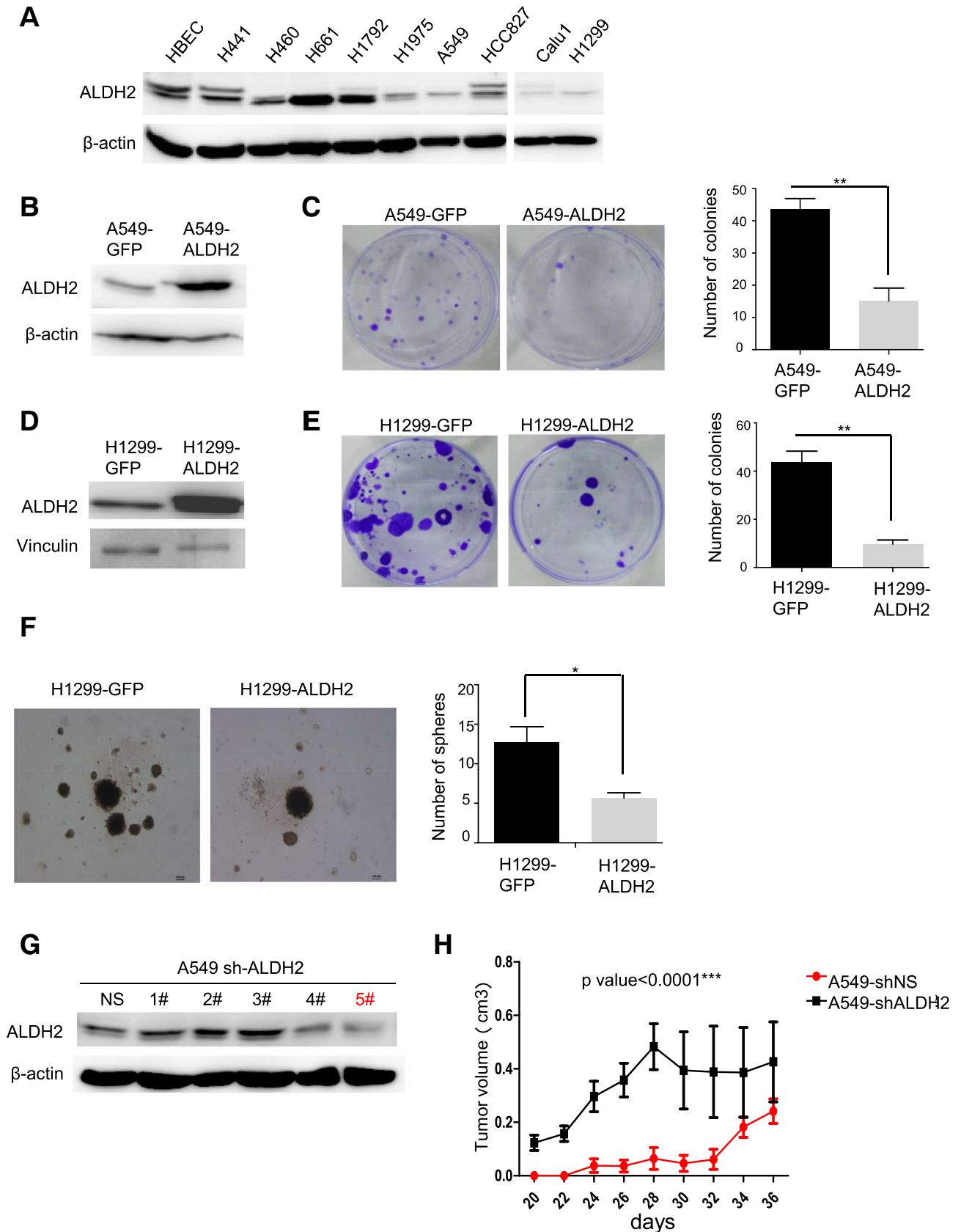
dehydrated using gradient Ethanol and xylene and sealed with neutral gum. Acquiesced images and analyzed by an inverted microscope.

Soft Agarose

2% agarose combined with RPMI-1640 containing 10% FBS (1:3 v/v; final concentration, 0.7%) was added to 24-well (0.5 ml per well), then the agarose solidified for 10 mins at 4°C. Lung adenocarcinoma cells (500 cells in 50 μl medium) were mixed in the culture medium containing 0 nM, 100 nM, 350 nM or 1 μM Alda-1 (MCE, HY-18936) and putted on the solidified agarose. On the top layer of the wells, 0.5 ml mixture of 2% agarose combined with RPMI-1640 containing 10% FBS (1:6 v/v; final concentration, 0.35%) along with matrigel (1:30 v/v) was added. The plate was incubated in 37°C /5% CO_2 incubator. After 2 weeks, established colonies were counted and photographed.

Immunohistochemistry (IHC)

The method was as described previously [13]. The γH2AX antibody was diluted to 1/500(v/v)in PBS.

Results

ALDH2 Repression is Associated with Poor Prognosis of Human Lung Adenocarcinoma

To investigate the relationship between ALDH2 and tumor progression, we analyzed the expression of ALDH2 mRNA in normal and tumor tissues from various cancer using the Gene Expression Profiling Interactive Analysis (GEPIA) dataset. The analysis showed that ALDH2 expression level was lower in tumor tissues as compared to normal tissues in most types of cancers, including lung adenocarcinoma (LUAD) and lung squamous cell carcinoma (LUSC) (Figure 1A). To validate the ALDH2 expression in human LUAD, we measured the mRNA levels of ALDH2 in 16 paired primary lung adenocarcinoma tissues and their adjacent normal tissues via Q-PCR analysis. The result showed that mRNA of ALDH2 was down-regulated in lung adenocarcinoma tissues as compared to their adjacent normal tissues in almost all of cases (Figure 1B). Next, we analyzed the survival rate of lung adenocarcinoma patients with low or high ALDH2 expression using the Cancer Genome Atlas (TCGA) dataset. Importantly, we found that the overall survival rate (%) of patients with ALDH2-low expression was significantly lower than that of patients with ALDH2-high expression (Figure 1C). The similar result was observed in analysis of dataset from the Human Protein Atlas (THPA) (Figure 1D). Moreover, repression of ALDH2 was associated with tumor stages, ALDH2 mRNA expression was significantly suppressed in tumor samples of tumor stage II to IV as compared to stage I (Figure 1E). These results suggest that ALDH2 repression is a predictive marker for the poor prognosis of lung cancer. We also analyzed ALDH2 protein expression via IHC staining from data of THPA. Consistent with mRNA expression, ALDH2 protein level is low in lung tumor

tissues as compared to that in normal lung tissues (data not shown). Taken together, ALDH2 repression is associated with the progression of human lung adenocarcinoma.

ALDH2 Overexpression Inhibits the Malignant Features of Lung Adenocarcinoma Cells

To determine the roles of ALDH2 in lung adenocarcinoma cells, next we examined ALDH2 expression in a set of human lung adenocarcinoma cell lines via Western blot analysis. ALDH2 expression was high in immortalized normal human lung epithelial cells (HBEC). But ALDH2 expression were down-regulated in most of human lung adenocarcinoma cell lines, including H1795, A549, HCC827, Calu-1, H1299, compared to that in HBEC; in comparison, only two human lung adenocarcinoma cell lines (H661, H1792) were expressed relatively high level of ALDH2 and two human lung adenocarcinoma cell lines (H441, H460) were expressed similar level ALDH2 as HBEC (Figure 2A). Thus, ALDH2 is down-regulated in most of lung adenocarcinoma cells.

To characterize the biological functions of ALDH2 in lung adenocarcinoma, we established ALDH2-overexpression transfectants in lung adenocarcinoma cell lines A549 and H1299 (Figure 2, B and D), or silenced ALDH2 using short hairpin (sh) RNA in A549 cells (Figure 2G). Then, we assayed the activities of these cell lines in colony formation, and 3D-sphere formation [14–17]. The results showed that A549-ALDH2 and H1299-ALDH2 cells exhibited significantly reduced colony forming capacity as compared to A549-GFP and H1299-GFP cells in colony formation assay (Figure 2, C and E). In addition, H1299-ALDH2 cells exhibited significantly reduced number of 3D-spheres as compared to H1299-GFP, although the size of 3D-spheres in two cell lines appeared similar (Figure 2F). Next, we investigated the biological functions of ALDH2 in vivo. A549-shNS and A549-shALDH2 cells ($1x10^6$) were subcutaneously injected into flanks of nude mice (n = 5). Tumor volumes were measured three times per week after tumor sizes were above 5x5 mm. The result showed that the tumor volumes of A549-shALDH2 were significantly larger than those of A549-shNS (Figure 2H). Taken together, these results suggest that ALDH2 overexpression inhibits the malignant features of lung adenocarcinoma cells, whereas ALDH2 repression enhances them.

ALDH2 Expression Inhibits the Stem-Like Features in Lung Adenocarcinoma Cells

To determine the mechanisms involved, we next examined the side population of A549-GFP, A549-ALDH2 and H1299-GFP, H1299-ALDH2 cells, the side population is widely considered as a stem cell-like population [18]. The results showed that the side population of A549-ALDH2 cells (4.79%) was decreased as compared to that of A549-GFP cells (8.76%) (Figure 3A). In this experiment, Ko143, an inhibitor of ABCG2, was used as a blocker. Similar results were obtained in the assay using Verapamil, an ABCB1 inhibitor, as blocker (Supplemental data Figure 1A). As the percentage of side population in H1299 cells is too low to detect, the analysis of side population was not performed in H1299 cell

Figure 2. ALDH2 over-expression suppresses the malignant features of lung adenocarcinoma cells. **A.** western blot analysis of ALDH2 expression in human lung adenocarcinoma cell lines as indicated. **B.** Western Blot analysis of ALDH2 expression in A549-GFP and A549-ALDH2 cells. **C.** Clone formation assay of A549-GFP and A549-ALDH2 cells. Histogram showed the colonies number in each group, *P < .05. **D.** Western blot showing ALDH2 expression in H1299-GFP, H1299-ALDH2 cells. **E.** Clone formation assay of H1299-GFP and H1299-ALDH2 cells. Histogram showed the colonies number in each group, *P < .05. **F.** Representative images and quantitative analysis of the 3D-sphere formation from the H1299-GFP, H1299-ALDH2 cells in 3D culture, *P < .05. **G.** Western blot showing ALDH2 expression in A549-shNS and A549-shALDH2 cells. **H.** Nude mice were injected with A549-shNS/shALDH2 cells ($1.0×10^6$ cells, n = 5) mixed with Matrigel, and the tumor volumes of each group were measured as indicated. P < .0001. Error bars represent SEM.
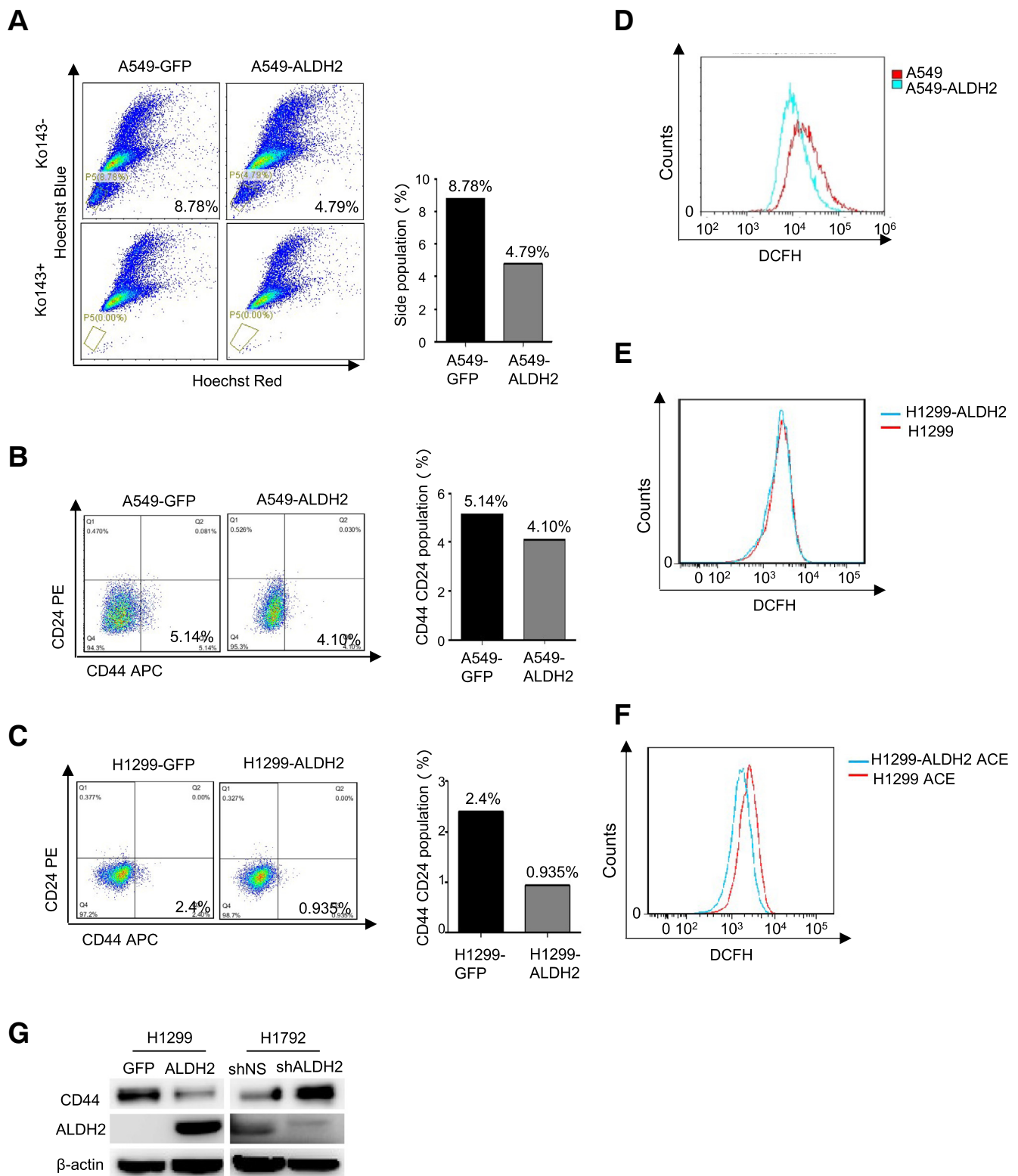
Figure 3. ALDH2 expression inhibits the stem-like features of lung adenocarcinoma cells. **A.** Identification of side population and main population in A549-GFP, A549-ALDH2 cells by FACS using Ko143 (5 μM) as an inhibitor of ABCG2 binding cassette. **B.** FACS analysis of the CD44+/C24- population of A549-GFP and A549-ALDH2 cells. **C.** FACS analysis of the CD44+/C24- population of H1299-GFP and H1299-ALDH2 cells. **D.** ROS analysis of A549, A549-ALDH2 cells by FACS. **E.** ROS analysis of H1299, H1299-ALDH2 cells by FACS. **F.** ROS analysis of H1299, H1299-ALDH2 cells treated with ACE for 2 days by FACS. **G.** Western blot analysis of CD44 in H1299-GFP cells, H1299-ALDH2 cells, H1792-shNS cells and H1792-shALDH2 cells.

line. For further characterization, CD44$^+$/CD24$^-$ population, which is widely considered as stem cell population in many cancers, including non-small-cell lung cancer, was also measured via Fluorescence Activated Cell Sorting (FACS) analysis [19,20]. The results showed that the CD44$^+$/CD24$^-$ population in A549-ALDH2 cells (4.10%) was reduced as compared to that of A549-GFP cells (5.14%) (Figure 3B). Similarly,

overexpression of ALDH2 in H1299 cells also decreased the CD44+/CD24− population (from 2.4% to 0.935%) (Figure 3C). Again, these results demonstrate that ALDH2 overexpression suppresses the stem cell-like population.

ROS affects stem cell-like population, whereas ALDH2 expression is implicated to downregulate ROS via detoxify ACE [21] [11], which in turn affect the stem cell-like population. So, we examined the ROS levels in A549 and A549-ALDH2 cells by FACS analysis. The results showed that the ROS level in A549-ALDH2 was significantly lower as compared to that in A549 (Figure 3D). Thus, ALDH2 expression suppresses ROS in A549 cells. The basal levels of ROS in H1299-ALDH2 and H1299 cells were similar (Figure 3E). However, when exogenous ACE was added to H1299 and H1299-ALDH2 cells, the ROS level was significantly lower in H1299-ALDH2 cells as compared to that in H1299 cells (Figure 3F). This suggests that H1299-ALDH2 cells have an enhanced capacity in detoxifying ACE-induced ROS, compared to H1299 cells. In conclusion, ALDH2 overexpression reduces ROS level and stem cell population in lung adenocarcinoma cells. Consistently, overexpression of ALDH2 inhibited CD44, the stem cell-like marker, in H1299-ALDH2 cells as compared to H1299-GFP cells in 3D culture, and depletion of ALDH2 increased CD44 expression in H1792-shALDH2 as compared to H1792-shNS cells (Figure 3G). Taken together, ALDH2 overexpression inhibits the stem-like features in lung adenocarcinoma cells.

ALDH2-Deficiency Leads to Accumulated ACE and Increased DNA Damage Both In Vitro and In Vivo

The major function of ALDH2 is to detoxify ACE [11]. Repression of ALDH2 is likely to result in accumulated ACE. To determine the effect of ALDH2 repression on endogenous ACE level, we measured the amount of ACE in A549-shNS and A549-shALDH2 cells. ALDH2 repression indeed resulted in an increased level of endogenous ACE in A549-shALDH2 cells as compared to that in control, A549-NS cells (Figure 4A). A recent study showed that increased level of ACE and ROS could induce DNA damage [11]. This suggests that increased endogenous ACE that resulted from ALDH2 repression could be a cause for increased genetic instability and malignant phenotypes. To determine this possibility, we examined DNA damages in A549-GFP and A549-ALDH2 cells via comet assay. The results showed that, although the basal level of DNA damage in A549-GFP and A549-ALDH2 cells were undetectable, addition of exogenous ACE induced intensive DNA damage in A549-GFP cells, but not A549-ALDH2 cells (Figure 4B). It is likely that ALDH2 overexpression detoxifies exogenous ACE and DNA damage in A549-ALDH2 cells.

To determine the cellular response to DNA damage, we examined γH2AX, a DNA-damage response protein, in these cells with or without treatment of ACE. Without treatment, A549-GFP and A549-ALDH2 cells, H1299-GFP and H1299-ALDH2 cells exhibited similar levels of γH2AX (Figure 4, C and D). However, under ACE treatment, A549-ALDH2 cells exhibited reduced γH2AX as compared to control cells A549-GFP (Figure 4C). Similar results were obtained in H1299-ALDH2 cells vs. H1299-GFP cells (Figure 4D). Taken together, ALDH2 overexpression confers the capacity to reduce ACE -mediated DNA damage.

To determine the roles of Aldh2 in vivo, we then measured the level of endogenous ACE in the lung tissues from wild-type (WT) and Aldh2-KO mice. As expected, the endogenous ACE level was significantly higher in Aldh2-KO mouse lungs than that in wild-type

ones (Figure 4E). To extend the functional relationship further, we next examined the endogenous ACE level of mouse lungs following intraperitoneal injection of Ethanol. Administration of exogenous Ethanol slightly increased endogenous ACE level in wild-type mice, suggesting that endogenous Aldh2 in wild-type mouse lungs is capable to detoxify ACE. Of notion, administration of exogenous Ethanol drastically increased the endogenous ACE level in Aldh2-KO mouse lungs (Figure 4E), indicating that Aldh2 deficiency leads to accumulated ACE in vivo. Thus, Aldh2 is essential for detoxification of ACE in mouse lungs in vivo. Consistent with in vitro assay, we examined γH2AX in lung tissues via Western blot and immunoblot analysis, the level of γH2AX was significantly increased in Aldh2-KO mouse lungs as compared to that in WT mouse lungs (Figure 4, F and G), suggesting an increased DNA damage response in Aldh2-KO mouse lungs. In addition, we found that the lung tissues from Aldh2-KO mice exhibited increased inflammatory characters compared to wild-type ones, including increased alveolar lesions and pulmonary edema, vascular wall thickness, perivascular leukocyte-rich inflammation and interstitial inflammation (Figure 4H). These changes suggest that Aldh2-KO mouse lungs suffer severe injury, probably oxidative stress or DNA damage stress. Moreover, these results suggest that Aldh2 deficiency leads to increased ACE and DNA damage in lung tissues in vivo. To correlate this observation, we analyzed the data from TCGA. We found that lung adenocarcinoma samples with low ALDH2 expression exhibited higher genetic mutations than those with high ALDH2 expression (Figure 4I). Taken together, ALDH2 overexpression confers the capacity to reduce ACE-mediated DNA damage.
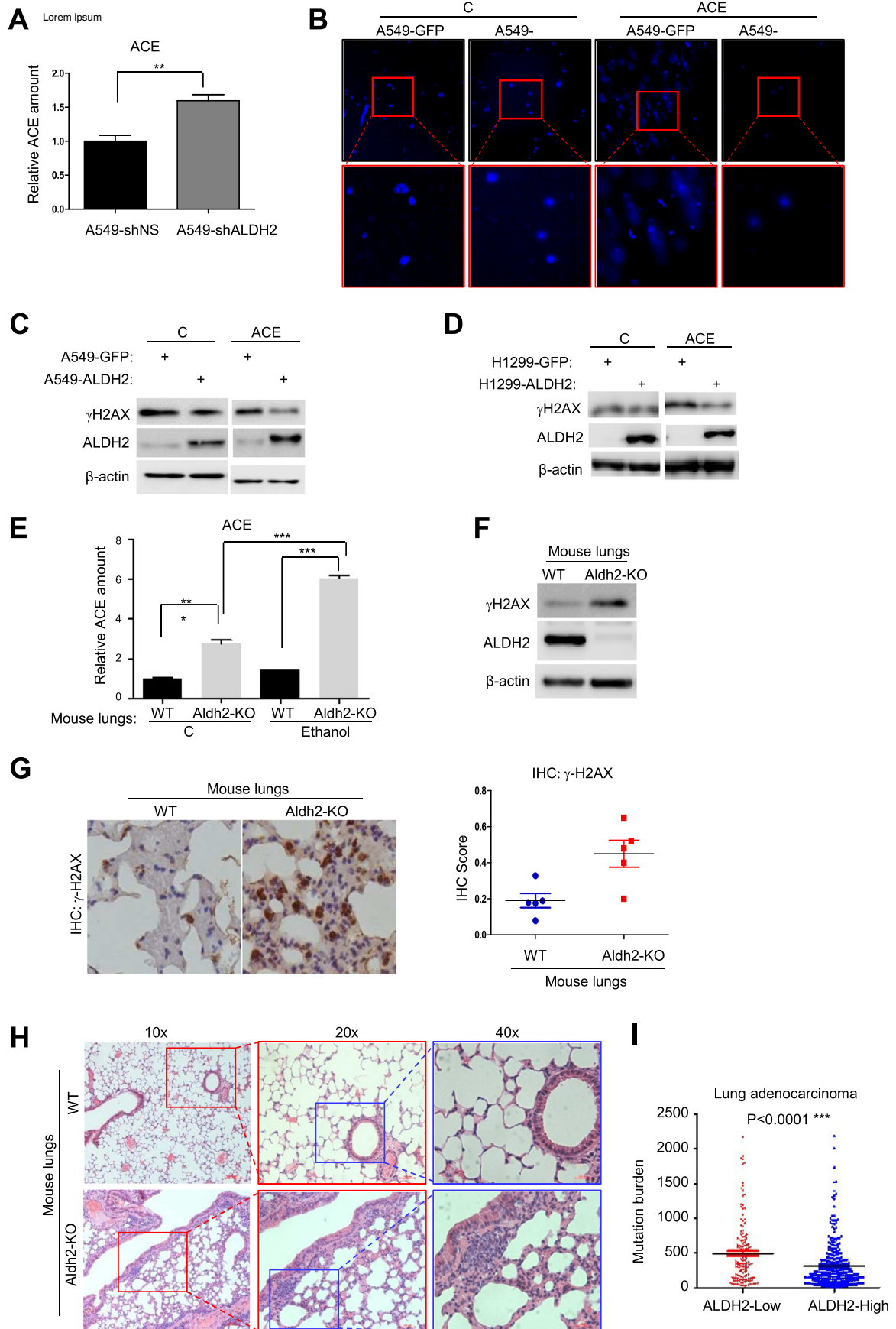
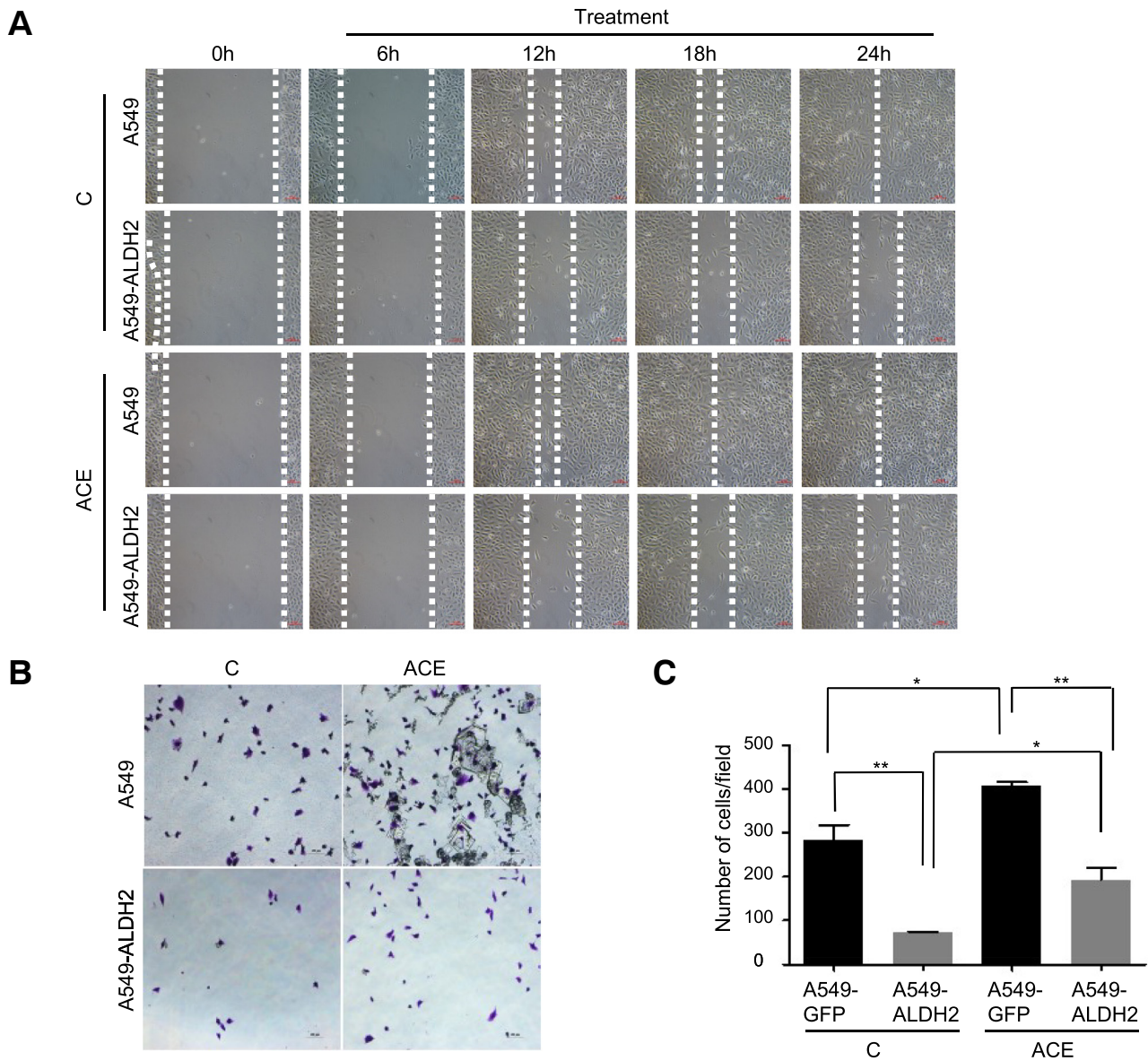### ACE Increases Migration in Lung Adenocarcinoma Cells

Recent evidences demonstrate that chromosome instability or DNA damage generate cytosolic DNA, further promotes the metastatic features of cancer cells [12]. Because ALDH2 deficiency leads to increased ACE and DNA damage, we assumed that these alterations effected metastatic capacity of lung adenocarcinoma cells. To determine this function, we compared the migration activities of A549-GFP and A549-ALDH2 cells in presence and absence of exogenous ACE. The results showed that A549-ALDH2 cells had reduced migration activity as compared to that of A549-GFP cells (Figure 5A). Importantly, addition of exogenous ACE increased the migration of A549 cells, but not A549-ALDH2 cells (Figure 5A), suggesting that A549-ALDH2 cells are capable to metabolize ACE whereas A549-GFP cells are not. Similar results were obtained by migration assay in transwell assay (Figure 5, B and C). These data indicate that ALDH2 dysfunction and exogenous ACE promote migration of lung adenocarcinoma cells, which could be abrogated by ALDH2 overexpression. Mechanistically, cytosolic DNA is implicated to promote metastasis in a STING-dependent manner [12]. Thus, we also examined STING expression and found that STING was decreased in A549-ALDH2 cells as compared to A549-GFP cells (Supplemental data Figure 1B). This implies that ALDH2 repression or ACE may affect migration in a DNA damage- and STING-dependent manner.

ALDH2 Agonist Alda-1 Inhibits the Malignant Features of Lung Adenocarcinoma Cells

Since ALDH2 overexpression inhibits the malignant features of lung adenocarcinoma cells, we then wondered whether activation of ALDH2 via its agonist could achieve the similar effects as ALDH2 overexpression. Next, we examined the effect of Alda-1 (N-(1,3-

Figure 5. ACE increases migration of lung adenocarcinoma cells. **A.** The migration capacity of A549-GFP and A549-ALDH2 cells that were treated with or without 1 mM ACE for two days was analyzed by a wound healing assay. **B. C.** Transwell assay for migration capacity of A549-GFP and A549-ALDH2 cells that were treated with or without 1 mM ACE. *$P < .05$.

benzodioxol-5-ylmethyl)-2,6-dichlorobenzamide), a selective agonist of ALDH2 [22], on lung adenocarcinoma cells. A549 cells were treated with Alda-1 at various concentrations for 2 days, followed by analysis of side population via FACS. The results showed that the cells treated with Alda-1, exhibited significantly reduced side population as compared to the untreated group (Figure 6A). Consistently, the ratio of CD44$^+$/CD24$^-$ population of H1299 was also significantly

reduced following Alda-1 treatment (Figure 6B). Thus, activation of ALDH2 by agonist Alda-1 inhibits the stem cell-like population in human lung adenocarcinoma cells.

Next, we examined the effect of Alda-1 on colony formation of A549 cells in soft agarose assay. The colony numbers of Alda-1-treated A549 cells in soft agarose were significantly reduced as compared to those of untreated ones (Figure 6C). Similar results were

Figure 4. ALDH2-deficiency leads to accumulated ACE and increased DNA damage. **A.** ACE quantification of A549-shNS and A549-shALDH2 cells by Mass spectrometry, *$P < .05$. **B.** Comet assay of A549-GFP and A549-ALDH2 cells that were treated with or without 4 mM ACE for 2 days. **C.** Western blot assay of γH2AX and ALDH2 in A549-GFP and A549-ALDH2 cells that were treated with or without 4 mM ACE for 2 days. **D.** Western blot assay of γH2AX and ALDH2 in H1299-GFP and H1299-ALDH2 cells that were treated with or without 4 mM ACE for 2 days. **E.** Relative quantification of ACE by Mass spectrometry of WT and Aldh2-KO mice lung tissues that were intraperitoneally injected with or without Ethanol (28% v/v in saline). Results are the mean (S.E.M.) of triplicate samples. t Test $P < .0001$. **F.** Western blot assay of γH2AX and ALDH2 in lung tissues of WT and Aldh2-KO mice. **G.** IHC staining and the score count of γH2AX in lung tissues from WT and Aldh2-KO mice. **H.** HE staining of lung tissues from WT and Aldh2-KO mice. **I.** Correlation analysis of ALDH2 expression and mutation burden in lung adenocarcinoma tissues using TCGA data.

observed in H1299 cells in 3D-sphere formation assay (Figure 6D). Of notion, Alda-1-induced inhibition on 3D-sphere formation was more drastic in H1299-ALDH2 cells than in H1299-GFP cells

(Figure 6D). This suggests that ALDH2 overexpression amplifies Alda-1-induced effects. To determine the effects on cell migration, we examined the migration of A549-GFP and A549-ALDH2 cells. Alda-
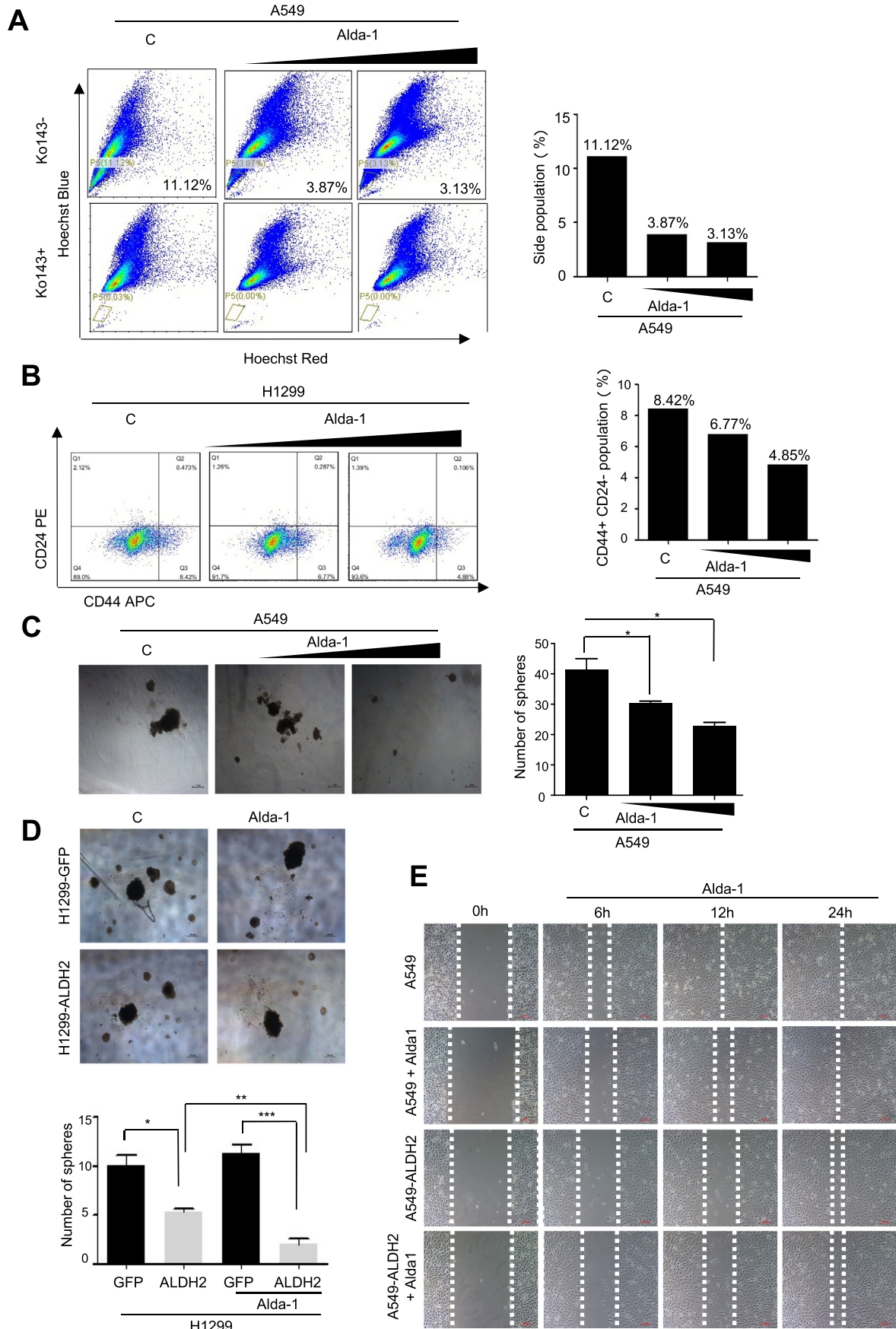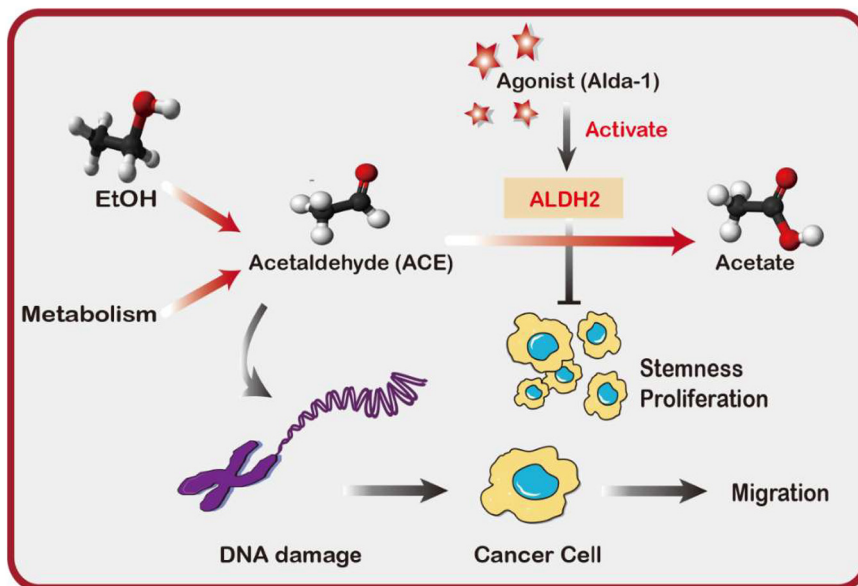
Figure 7. Graphic abstract representing a proposed model of ALDH2 repression-mediated tumor progression.

1 treatment inhibited the migration of A549-GFP cells (Figure 6E), suggesting activation of endogenous ALDH2 by agonist Alad-1 inhibits the migration of A549 cells. However, Alda-1 induced effect was not further enhanced in A549-ALDH2 cells (Figure 6E). Taken together, these observations demonstrate that activation of ALDH2 by agonist, acting similarly as ALDH2 overexpression, inhibits the malignant features of lung adenocarcinoma cells.

Discussion

In this study, we found that ALDH2 was suppressed in human lung adenocarcinoma. ALDH2 suppression led to accumulated ACE, which induced DNA damage and promoted the malignant features in lung adenocarcinoma cells. Moreover, accumulated ACE and increased DNA damage have been identified in Aldh2-KO mouse lung tissues in vivo. Importantly, activation of ALDH2 with its agonist inhibited the malignant features of lung adenocarcinoma cells. Thus, targeting ALDH2 may provide a novel strategy for lung cancer therapy.

ALDH2 is mainly responsible for metabolism of ACE to acetate [23]. ACE is a highly reactive compound that could interact with DNA to form many kinds of adducts [24], leading to genetic mutations for carcinogenesis. However, the research about ALDH2 on tumor progression is limited. A recent study suggests that ALDH2 functions as an inhibitor of the metastasis in liver cancer cells [9]. The function and mechanism of ALDH2 and ACE on lung cancer progression has not been studied thoroughly. In this study, we firstly found that the malignant features of ALDH2-low expressing lung

adenocarcinoma cells could be reversed by ALDH2 overexpression. Biologically, ALDH2 reduction not only increased the proliferation and stemness of lung adenocarcinoma cells, but also enhanced DNA damage and migration. This is important for tumor progression since tumor relapse, drug-resistance and metastasis are strongly correlated with increased cancer stem cell or the stem-like features [10,25]. It also has been reported that the increased ratio of XRCC1, a base excision repair protein, and ALDH2 levels was indicative for poor overall survival in lung and liver cancer patients, but not those with esophageal cancers [26]. This suggests that ALDH2 dysfunction is important in lung tumor and liver tumor although not in esophageal cancer. Thus, the oncogenic roles of ALDH2 dysfunction may be cellular context-dependent.

Chromosomal instability is a hallmark of cancer. A recent study shows that chromosomal instability promotes metastasis by sustaining a tumor cell-autonomous response to cytosolic DNA [12]. In this study, we found that ALDH2 deficiency led to increased ACE and DNA damage in lung adenocarcinoma cells. Moreover, exogenous ACE significantly increases the migration capacity of lung adenocarcinoma cells. Importantly, a functional link from accumulated ACE to increased DNA damage has been identified in Aldh2-KO mouse lungs in vivo. Consistent with increased DNA damages, Aldh2-KO mouse lungs exhibited drastically increased inflammation, injury as compared to those in wild-type ones. In addition, the same study indicates that chromosomal instability and DNA damage lead to ruptured genomic DNA spilling into the cytosol, it further promotes

Figure 6. ALDH2 agonist Alda-1 alleviates malignant features of lung adenocarcinoma cells. **A.** Identification of side population and main population in A549 cells that were treated with Alda-1for different concentrations (0 nM, 350 nM,5 μM) by FACS using Ko143 (5 μM) as an inhibitor of ABCG2 binding cassette. **B.** Identification of CD44+/C24- population in H1299 cells treated with Alda-1 for different concentrations (0 nM, 100 nM, 1 μM) by FACS analysis. **C.** Representative images and quantitative analysis of colonies formed from A549 cells that were treated with different concentrations of Alda-1 (0 nM, 100 nM, 1 μM) in soft agarose. Results are the mean (S.E.M.) of triplicate samples. **D.** Representative images and quantitative analysis of 3D-spheres formed from H1299-GFP and H1299-ALDH2 cells that were treated with or without 1 μM Alda-1. Results are the mean (S.E.M.) of triplicate samples. **E.** The migration behavior of A549-GFP and A549-ALDH2 cells that were treated with different concentrations of Alda-1 (0 nM, 350 nM, 1 μM) was analyzed by a wound healing assay.

metastasis in a STING-dependent manner [12]. In our study, we also observed the reduction of STING in A549-ALDH2 cells as compared to A549-GFP cells. However, whether ALDH2 and ACE affects the migration of lung adenocarcinoma cells via DNA damage-dependent and STING-dependent pathway requires further determination.

In this study, administration of ALDH2 activator Alda-1 [22] reduced the stem-like and metastatic features of lung adenocarcinoma cells. The observation is expected, since it is consistent with the roles of ALDH2 in lung adenocarcinoma cells. Interestingly, disulfiram, an ALDH2 inhibitor, has also been found to inhibit the proliferation of variety tumors [27–29]. This observation appears to be contradictive to what is studied in this article. The discrepancy may be due to the following reasons: 1. Cancer cells may be addictive to certain oncogenic signaling, such as ACE and ROS in ALDH2-deficient cancer cells. Inhibition of ALDH2 by disulfirm could further increase the level of ROS, which could be highly cytotoxic in ALDH2-deficient cancer cells. However, normal cells are expressing relatively high ALDH2, which is sufficient for ACE metabolism. Thus, the effect of disulfirm in normal cells is limited. 2. Disulfiram exerts tumor inhibition effects by forming diethyldithiocarbamate (Cu (DETC)2) complex. Whether the complex plays its role via the regulation to ALDH activity is still unknown. 3. Disulfiram is an activity inhibitor of various subtypes of ALDH, not specifically act on ALDH2. It is therefore possible that disulfiram exert its tumor inhibition effects via action on other subtypes. However, these hypotheses need more researches to verify.

In summary, we propose that ALDH2 repression promote proliferation and stemness of lung adenocarcinoma cells. It also leads to ACE accumulation, which induces DNA damage and metastatic features in lung adenocarcinoma cells (Figure 7).

Supplementary data to this article can be found online at https://doi.org/10.1016/j.neo.2019.03.008.

Declarations of Interest
None.

Acknowledgments

References
[1] Chen W, Zheng R, Baade PD, Zhang S, Zeng H, Bray F, Jemal A, Yu XQ, and He J (2016). Cancer statistics in China, 2015. *CA Cancer J Clin* **66**(2), 115–132.

[2] Siegel RL, Miller KD, and Jemal A (2015). Cancer statistics, 2016. *CA Cancer J Clin* **60**(5), 277–300.

[3] Robbiano L, Baroni D, Novello L, and Brambilla G (2006). Correlation between induction of DNA fragmentation in lung cells from rats and humans and carcinogenic activity. *Mutat Res* **605**(1), 94–102.

[4] Á-A SM, Fernández-Somoano A, Navarrete-Muñoz EM, Vioque J, and Tardón A (2017). Effect of alcohol and its metabolites in lung cancer: CAPUA study. *Med Clin (Barc)* **148**(12).

[5] Voulgaridou GP, Anestopoulos I, Franco R, Panayiotidis MI, and Pappa A (2011). DNA damage induced by endogenous aldehydes: Current state of knowledge. *Mutat Res* **711**(1–2), 13–27.

[6] Chang JS, HJChen CH (2017). ALDH2 polymorphism and alcohol-related cancers in Asians: a public health perspective. *J Biomed Sci* **24**(21), 19.

[7] Chen CH, Ferreira JC, Gross ER, and Mochlyrosen D (2014). Targeting aldehyde dehydrogenase 2: new therapeutic opportunities. *Physiol Rev* **94**(1), 1.

[8] Adams KE and Rans TS (2013). Adverse reactions to alcohol and alcoholic beverages. *Ann Allergy Asthma Immunol* **111**(6), 439–445.

[9] Hou G, Chen L, Liu G, Li L, Yang Y, Yan HX, Zhang HL, Tang J, Yang YC, and Lin X (2017). Aldehyde dehydrogenase-2 (ALDH2) opposes hepatocellular carcinoma progression by regulating AMP-activated protein kinase signaling in mice. *Hepatology* **65**(5), 1628.

[10] Moreb JS, Ucar D, Han S, Amory JK, Goldstein AS, Ostmark B, and Chang LJ (2012). The enzymatic activity of human aldehyde dehydrogenases 1A2 and 2 (ALDH1A2 and ALDH2) is detected by Aldefluor, inhibited by diethylamino-benzaldehyde and has significant effects on cell proliferation and drug resistance. *Chem Biol Interact* **195**(1), 52–60.

[11] Garaycoechea JI, Crossan GP, Langevin F, Mulderrig L, Louzada S, Yang F, Guilbaud G, Park N, Roerink S, and Nikzainal S (2018). Alcohol and endogenous aldehydes damage chromosomes and mutate stem cells. *Nature* **553**(7687), 171–177.

[12] Bakhoum SF, Ngo B, Laughney AM, Cavallo JA, Murphy CJ, Ly P, Shah P, Sriram RK, Watkins T, and Taunk NK (2018). Chromosomal instability drives metastasis through a cytosolic DNA response. *Nature* **553**(7689).

[13] Lin X, Zhong S, Ye X, Liao Y, Yao F, Yang X, Sun B, Zhang J, Li Q, and Gao Y (2014). EGFR phosphorylates and inhibits lung tumor suppressor GPRC5A in lung cancer. *Mol Cancer* **13**(1), 1–12.

[14] Yamada KM and Cukierman E (2007). Modeling tissue morphogenesis and cancer in 3D. *Cell* **130**(4), 601–610.

[15] Gibbons JA, Kanwar RK, and Kanwar JR (2011). Lactoferrin and cancer in different cancer models. *Front Biosci* **3**, 1080–1088.

[16] Serebriiskii I, Castellócros R, Lamb A, Golemis EA, and Cukierman E (2008). Fibroblast-derived 3D matrix differentially regulates the growth and drug-responsiveness of human cancer cells. *Matrix Biol* **27**(6), 573–585.

[17] Kim JB, Stein R, and O'Hare MJ (2004). Three-dimensional in vitro tissue culture models of breast cancer — a review. *Breast Cancer Res Treat* **85**(3), 281–291.

[18] Ho MM, Ng AV, Lam S, and Hung JY (2007). Side population in human lung cancer cell lines and tumors is enriched with stem-like cancer cells. *Cancer Res* **67**(10), 4827–4833.

[19] Leung EL, Fiscus RR, Tung JW, Tin VP, Cheng LC, Sihoe AD, Fink LM, Ma Y, and Wong MP (2010). Non-small cell lung cancer cells expressing CD44 are enriched for stem cell-like properties. *PLoS One* **5**(11)e14062.

[20] CHSMertins SD, Busch JI, Gowens M, Scudiero DA, Burkett MW, Hite KM, Alley M, Hollingshead M, and Shoemaker RH (2010). Complex display of putative tumor stem cell markers in the NCI60 tumor cell line panel † ‡ §. *Stem Cells* **28**(4), 649–660.

[21] Amanuma Y, Ohashi S, Itatani Y, Tsurumaki M, Matsuda S, Kikuchi O, Nakai Y, Miyamoto S, Oyama T, and Kawamoto T (2015). Protective role of ALDH2 against acetaldehyde-derived DNA damage in oesophageal squamous epithelium. *Sci Rep* **5**, 14142.

[22] Sun L, Ferreira JC, and Mochlyrosen D (2011). ALDH2 activator inhibits increased myocardial infarction injury by nitroglycerin tolerance. *Sci Transl Med* **3**(107)107ra111.

[23] Park JY, Matsuo K, Suzuki T, Ito H, Hosono S, Kawase T, Watanabe M, Oze I, Hida T, and Yatabe Y, et al (2010). Impact of smoking on lung cancer risk is stronger in those with the homozygous aldehyde dehydrogenase 2 null allele in a Japanese population. *Carcinogenesis* (4), 660–665.

[24] Hsu-Sheng Y, Tsunehiro O, Toyohi I, Kyoko K, Thi-Thu-Phuong P, Masayuki T, and Toshihiro K (2010). Formation of acetaldehyde-derived DNA adducts due to alcohol exposure. *Chem Biol Interact* **188**(3), 367–375.

[25] Kim J, Chen CH, Yang J, and Mochlyrosen D (2017). Aldehyde dehydrogenase 2*2 knock-in mice show increased reactive oxygen species production in response to cisplatin treatment. *J Biomed Sci* **24**(1), 33.

[26] Chen X, Legrand AJ, Cunniffe S, Hume S, Poletto M, Vaz B, Ramadan K, Yao D, and Dianov GL (2018). Interplay between base excision repair protein XRCC1 and ALDH2 predicts overall survival in lung and liver cancer patients. *Cell Oncol* , 1–13.

[27] Wickström M, Danielsson K, Rickardson L, Gullbo J, Nygren P, Isaksson A, Larsson R, and Lövborg H (2007). Pharmacological profiling of disulfiram using human tumor cell lines and human tumor cells from patients. *Biochem Pharmacol* **73**(1), 25–33.

[28] Conticello C, Martinetti D, Adamo L, Buccheri S, Giuffrida R, Parrinello N, Lombardo L, Anastasi G, Amato G, and Cavalli M (2012). Disulfiram, an old drug with new potential therapeutic uses for human hematological malignancies. *Int J Cancer* **131**(9), 2197–2203.

[29] Shian SG, Kao YR, Wu FY, and Wu CW (2003). Inhibition of invasion and angiogenesis by zinc-chelating agent disulfiram. *Mol Pharmacol* **64**(5), 1076–1084.